Constraining sterile neutrino oscillation with MicroBooNE data

Third Year Lab Report

Lewis Dean
Department of Physics and Astronomy, University of Manchester
(Experiment performed in collaboration with Robin de Freitas)
(Dated: October 13, 2024)

The existence of sterile neutrinos, within a 3+1 model, would influence muon neutrino oscillation. Hence, it could explain the low energy excesses observed in the LSND and MiniBooNE experiments. Data from the MicroBooNE detector was fitted to oscillated Monte Carlo simulated events, leading to the exclusion of possible 3+1 oscillation parameters . At the 99% confidence level, this oscillation analysis only excluded a small region of parameter space which was consistent with the LSND anomaly. With the same confidence, none of the possible MiniBooNE oscillation parameters were excluded here.

1. INTRODUCTION

One of the mysteries Fermilab's MicroBooNE experiment set to elucidate was whether the observed low energy excess of electron-type neutrino interactions could be explained by the existence of a sterile neutrino. This would be a fourth neutrino flavour that does not undergo weak interactions. In 2001, the Liquid Scintillator Neutrino Detector (LSND) showed an excess of anti-electron neutrino events, induced by an anti-muon neutrino beam [1]. Their frequency was inexplicable by beam impurities, and most importantly by the current 3-neutrino model. Further research into this anomaly was undertaken by MiniBooNE, with the experiment unable to reject the possibility of a sterile neutrino explaining its own low energy excess of electron neutrinos. However, the more sophisticated apparatus implemented at MicroBooNE should allow for further constraint of the oscillatory behaviour a sterile neutrino could viably demonstrate.

2. THEORY OF NEUTRINO OSCILLATION

The advent of neutrino oscillations served to explain the solar neutrino problem. This was the deviation of the experimentally observed neutrino flux, received by Earth due to stellar nucleosyntehsis, from that which was theoretically predicted. Considering neutrino oscillation resolves this discrepancy because, although neutrinos are produced of a definite flavour, the mass eigenstates that constitute said flavour become out of phase as they propagate through space. Consequently, a neutrino interacting some distance away from its creation point has a finite probability of doing so as a different flavour. Note that one can transform between the mass and flavour eigenbases of the 3ν model via the PMNS matrix,

$$\begin{bmatrix}\nu_e\\ \nu_\mu\\ \nu_\tau\end{bmatrix} = \mathbf{U}_{\text{PMNS}} \begin{bmatrix}\nu_1\\ \nu_2\\ \nu_3\end{bmatrix}, \tag{1}$$

with the right-hand side of this equation denoting a transformation of the mass eigenbasis to its flavour eigenbasis (electron, muon, tau), shown on the left-hand side. This matrix encodes the mixing angles, $\theta_{\alpha\beta}$, between α and β flavoured neutrinos; these parameters define the amplitude of mutual oscillation probabilities. Besides this, the difference between squared mass eigenvalues also influences the oscillation probability. Specifically, a large mass difference increases the rate in which a flavour's mass eigenstates become out of phase, reducing the distance required for neutrino oscillation to become significant. For short baseline neutrino experiments, like MicroBooNE, one can make a two-flavour approximation with the oscillation probability,

$$P(\nu_\mu \to \nu_\tau) = \sin^2(2\theta)\sin^2\Delta_{12}\,, \tag{2}$$

$$\Delta_{12} = 1.27\,\frac{\Delta m^2_{12} L\,(\text{eV}^2)(\text{km})}{E\,(\text{GeV})}\,, \tag{3}$$

wherein Δm^2_{21} is the difference in the squared first and second mass eigenvalues. The baseline, L, is the distance travelled since the neutrino's creation and E is its energy. All mixing angles are equivalent within this approximation, thus simply labelled θ.

3. EXPERIMENTAL METHOD

3.1. MicroBooNE detector

MicroBooNE makes use of Fermilab's Booster Neutrino Beam (BNB). To create this beam, protons are accelerated towards a Beryllium target. Their collisions produce charged pions and kaons, separated by their sign via magnetic horns [2]. The positive and negative mesons respectively have the primary decay modes $\mu^+\nu_\mu$ and $\mu^-\bar{\nu}_\mu$. The two beams pass through solid ground, filtering out the charged leptons, leaving behind beams composed exclusively of neutrinos. For the data discussed here, the ν_μ beam was incident upon MicroBooNE's Liquid Argon Time Projection Chamber (LArTPC).

When neutrinos enter the LArTPC, they can interact with Argon nuclei. The dominant ν_μ interaction channel at these energies is their charged current (CC) interaction with neutrons, producing a proton and muon, as shown in Figure 1. Around the interaction vertex, scintillation photons are emitted and soon after detected by an array of photomultiplier tubes (PMTs), signposting the occurrence of a neutrino interaction [2]. The muon and proton, being charged, ionise electrons as they propagate through the Argon. Due to an electric field placed around the chamber, ionised electrons drift towards 3 wire planes at the anode, triggering electrical signals. These signals, in conjunction with the scintillation data, imply the drift-time for these electrons to reach the wire planes; therefore, a 3D reconstruction of the muon and proton's tracks can be generated.

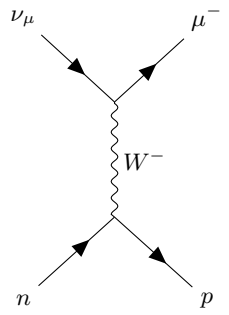

FIG. 1. Feynman diagram of the signal event in this analysis. This is the ν_μCC interaction with Argon neutrons.

3.2. Monte-Carlo simulation of detector events

To test how current theories explain real-world observations, multiple pieces of software are combined to produce Monte Carlo (MC) simulations of what wire plane and PMT signals MicroBooNE would detect, in the absence of neutrino oscillation. Then, an oscillation analysis can be applied, in which some ν_μ disappear before interaction, with the aim of finding oscillation parameters that best fit the experimental data. These simulated events have definite energies and baselines, whereas real events can only have these approximated by reconstruction algorithms. The MC data had external (EXT) data added which is real-world data, recorded when the beam was off, accounting for any non-simulated background events. The "MC_EXT" data is inputted to the same reconstruction algorithms used at MicroBooNE. The identified track features can be noted for each event type, and possible relationships between them discovered, with the expectation being that the same relationships exist within real-world events.

3.3. Signal event isolation

Crucially, the signal event is not the most abundant interaction within the detector's active volume. Most neutrinos pass through the detector without interacting, but atmospheric muons produce many detector events. The beam is spilled in 1.6 μs intervals [2], restricting the time domain in which scintillation data most likely describes a neutrino interaction, yet "cosmics" still contribute to background noise. Moreover, the beam contains minor ν_e impurities, due to alternate decay modes of the mesons, as well as the fact both neutrino types can undergo neutral-current (NC) interactions. These other events must be seperated from our signal prior to further analysis.

One approach to this is to train a machine learning model on the MC_EXT data, where the true event classifications are known. Thus, they can be used to assess the model's performance. Both random decision forests and boosted decision trees were implemented here, with the goal of ranking the importance of different track features towards successfully classifying event types. The model hyperparameters were tuned for optimising the accuracy score achieved on test data, with the random decision forest and gradient boosting classifiers having accuracies of 55.8% and 62.2% respectively. The most important track features were considered first when making selection cuts to data.

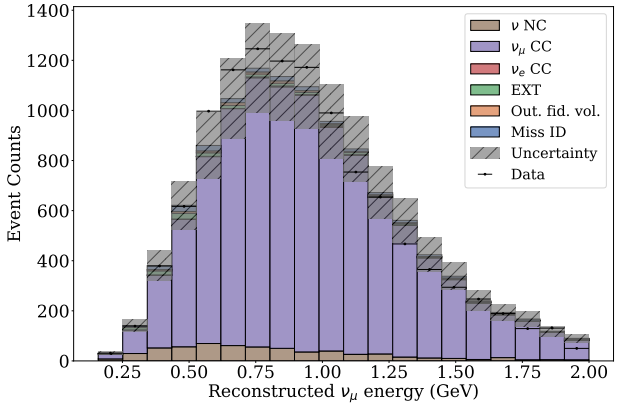

FIG. 2. A stacked histogram of energies for post-selection-cut MC events. The legend specifies the different interaction categories, where "data" is that observed at MicroBooNE and "uncertainty" is that given in equation (4).

The selection cuts made focused on three track features: energy, fiducial volume and topological score, τ. The reconstructed energy was restricted to below 2 GeV as failures in event reconstruction were labelled with non-physically high energies. Any track features within the outer fiducial volume led to that event being cut, as cosmic-induced interactions are more likely in that region. Finally, τ is a machine learning score characterising the event's topology. Scores closer to 1 are more neutrino-like, whilst those closer to 0 resemble more so cosmic interactions. Hence, events with $\tau < 0.6$ were cut. The quality of selection cuts were assessed using their efficiency and purity. Efficiency is defined as the fraction of events remaining after selection cuts are made. Purity is the fraction of post-cut events which are the desired signal event. These cuts ultimately led to an efficiency of 11.4% and a purity of 90.3%.

4. OSCILLATION ANALYSIS

One can extract neutrino oscillation parameters via an oscillation analysis. This involves scaling the counts that ν_μ MC events contribute to an energy histogram's bins by their associated survival probabilities, $1 - P(\nu_\mu \to \nu_\tau)$. The best fit θ and Δm^2_{12} are those that minimise the χ^2 statistic between the oscillated MC_EXT data and real MicroBooNE data. Figure 2 illustrates such a histogram, prior to oscillation analysis, wherein the efficacy of the selection cuts is made evident.

4.1. Error calculations

The dominant errors here are systematic, contributing a flat 15% uncertainty to each bin. One source of this is the capture of ionised electrons by active volume impurities, more electronegative than Argon, erasing wire plane data that would otherwise aid event reconstruction [3]. In addition, the counts, C, observed per bin are regarded as Poisson distributed, leading to an error of $\sqrt{C}$. Propagating these using fractional quadrature yields a total bin error, ΔC, of,

$$\Delta C = C\sqrt{0.15^2 + \frac{1}{C}}\,. \tag{4}$$

These errors were used within χ^2 calculations. Moreover, on a χ^2 contour plot, spanned by the oscillation parameters, contours of particular χ^2 values can be added; these define regions that one can say, with varying confidences, the true oscillation parameters lie within. The contours are defined by the associated critical χ^2 values for a fit with 2 degrees of freedom.

4.2. Closure test

To ensure successful oscillation analysis implementation, a closure test was performed. This used MC_EXT data manually oscillated with specifically chosen parameters. The χ^2 between fitted and manually oscillated data was minimised. Since both were oscillated MC_EXT data, the fit should be almost perfect, with any deviation due to uncut, non-signal events. The obtained χ^2_{min} was 0.58, and thus the closure test was deemed successful.

4.3. 3+1 neutrino model fit

To explore possible oscillation parameters for a sterile neutrino, the two-flavour approximation parameters, associated with ν_μ survival, were mapped to the ν_e appearance parameter space. This was because the latter space was restricted in earlier LSND and MiniBooNE analyses. Equation (1) can be modified for a 4x4 lepton mixing matrix, including oscillation into a fourth, sterile, state. From this, it is possible to derive the following mixing angle relation:

$$\sin^2(2\theta_{\mu e}) = \left(1 - \sqrt{1 - \sin^2(2\theta_{\mu\mu})}\right) \times \left(1 - \sqrt{1 - \sin^2(2\theta_{ee})}\right). \quad (5)$$

$\theta_{\mu\mu}$ is the best fit mixing angle when MC events are oscillated with the ν_μ survival probability. θ_{ee} determines ν_e survival and $\theta_{\mu e}$ specifies $\nu_\mu \rightarrow \nu_e$ oscillation. Given $\sin^2(2\theta_{ee}) = 0.24$ [4], equation (5) provides the desired mapping between parameter spaces, with Δm^2_{12} becoming Δm^2_{14}.

The red dot within Figure 3 shows the best fit ν_e appearance oscillation parameters for the 3+1 model. The contours included are for 90%, 95% and 99% confidence levels. These indicate the confidence in which one can say, to the left of that contour, the true $\left(\sin^2(2\theta_{\mu e}),\ \Delta m^2_{14}\right)$ pair would need to lie. The contours overlay shaded parameter space regions which highlight the possible 3+1 parameters for elucidating the low energy excesses of LSND and MiniBooNE. Even with 90% confidence, the analysis performed here is unable to exclude any of the parameter space proposed by the MiniBooNE experiment. At the 99% confidence level, a tiny region of the LSND data can be excluded where $\sin^2(2\theta_{\mu e}) \sim 10^{-2}$ and $\Delta m^2_{14} \sim 4$.

5. EVALUATION

The selection cuts here had low efficiency, as cutting non-physically high energies removed 85% of MC simulated events. Thus, improving MicroBooNE's reconstruction algorithms would allow more detector events to be analysed. The number of ν_μ events recorded per unit time could be increased with a higher BNB flux, as well as thicker detector casing to further shield from cosmics, reducing the need for brief beam spills. The primary non-signal events in figure 2 are NC neutrino interactions. Therefore, machine learning could be employed to find novel NC orientated cuts. Increasing purity and the total histogram counts would expand Figure 3's exclusion zones, allowing more LSND/MiniBooNE parameter pairs to be rejected.

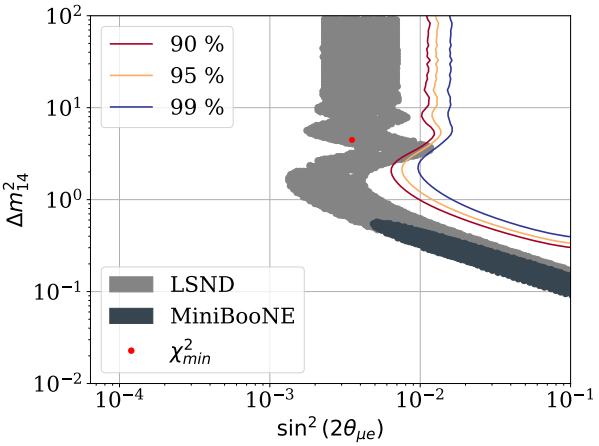

FIG. 3. Contour plot depicting exclusion zones of various confidence levels alongside the LSND/MiniBooNE parameter space restrictions. The χ^2 was minimised using the L-BFGS-B algorithm.

6. CONCLUSION

To conclude, this 3+1 oscillation analysis only rejected a small portion of LSND parameters, and no MiniBooNE parameters, at the 99% confidence level. The dominant source of error was systematic uncertainty, with one source being Argon impurities. Perhaps, more frequent cycling of the detector's Argon could reduce interference between previously ionised atoms and the particle tracks of subsequent interactions. This would facilitate more reliable event reconstructions.

[1] S. N. Gninenko, LSND/MiniBooNe excess events and heavy neutrino from and K decays, Physical Review D **83**, 093010 (2011).
[2] D. Kaleko, *MicroBooNE: The Search For The MiniBooNE Low Energy Excess*, Tech. Rep. FERMILAB-THESIS–2017-12, 1354863 (2017).
[3] MicroBooNE, *Measurement of the Electronegative Contaminants and Drift Electron Lifetime in the MicroBooNE Experiment*, Tech. Rep. FERMILAB-MICROBOONE-NOTE-1003-PUB, 1573040 (2016).
[4] MicroBooNE-Collaboration, First constraints on light sterile neutrino oscillations from combined appearance and disappearance searches with the MicroBooNE detector, Physical Review Letters **130**, 011801 (2023).